International Journal of Thermofluids 9 (2021) 100057

Contents lists available at ScienceDirect

International Journal of Thermofluids

journal homepage: www.elsevier.com/locate/ijtf

Impact of local secondary gas addition on the dynamics of self-excited ethylene flames

Taaha Hussain[a], Midhat Talibi*,[a], Ramanarayanan Balachandran[a]

Department of Mechanical Engineering, University College London, Torrington Place, London, WC1E 7JE, United Kingdom

ARTICLE INFO

Article History:
Received 26 August 2020
Revised 20 November 2020
Accepted 24 November 2020
Available online 28 November 2020

Keywords:
Lean burn
Combustion instability
Gas turbine
NOx Emissions
Hydrogen
Self excited oscillations

ABSTRACT

Advanced combustion strategies for gas turbine applications, such as lean burn operation, have been shown to be effective in reducing NOx emissions and increasing fuel efficiency. However, lean burn systems are susceptible to thermo-acoustic instabilities which can lead to deterioration in engine performance. This paper will focus on one of the common industrial techniques for controlling combustion instabilities, secondary injection, which is the addition of small quantities of secondary gas to the combustor. This approach has often been employed in industry on a trial-and-error basis using the primary fuel gas for secondary injection. Recent advances in fuel-flexible gas turbines offers the possibility to use other gases for secondary injection to mitigate instabilities. This paper will explore the effectiveness of using hydrogen for this purpose.

The experiments presented in this study were carried out on a laboratory scale bluff-body combustor consisting of a centrally located conical bluff body. Three different secondary gases, ethylene, hydrogen and nitrogen, were added locally to turbulent imperfectly-premixed ethylene flames. The total calories of the fuel mixture and the momentum ratio were kept constant to allow comparison of flame response. The heat release fluctuations were determined from the OH* chemiluminescence, while the velocity perturbations were estimated from pressure measurements using the two-microphone method. The results showed that hydrogen was the most effective in reducing the magnitude of self-excited oscillations. Nitrogen had negligible effect, while ethylene only showed an effect at high secondary flow rates which resulted in sooty flames.

1. Introduction

While lean burn operation in gas turbine combustion is beneficial in reducing emissions of nitrogen oxides (NOx), these systems are susceptible to thermo-acoustic oscillations, commonly known as combustion instabilities [1–5]. These instabilities are caused by unsteady combustion which can alter the heat release rate, and even travel further upstream the combustor and interfere with the air/fuel mixing process [6]. These instabilities are problematic as they result in severe vibrations of the combustor walls, excessive heat transfer, flame blow-off, unacceptable noise levels and component wear, potentially leading to a complete failure of the system [7–11].

Studying the interactions between large scale coherent structures (vortices), caused by hydrodynamic instabilities or acoustic disturbances, and flames is crucial to improve our understanding of fundamental mechanisms in turbulent combustion and combustion instabilities. Flame-vortex interactions can be used to analyse phenomena relating to the structure of the flame when it is wound up by a vortex (also known as flame roll-up), formation of a central core, secondary vorticity generation, quenching of the reaction zone, ignition dynamics, mixing and combustion enhancement [12–15]. In order to determine correlations between flame and flow dynamics, flame-vortex interactions have been studied in several different configurations: counterflow diffusion flames [16,17], turbulent swirl flames [18–22], propagating flat flames [23,24] and turbulent jet flames [25,26]. Optical diagnostic techniques, such has high repetition rate PIV (particle image velocimetry) and PLIF (planar laser induced fluorescence), have recently been used to study transient phenomena caused by vortex structures, such as lean blowout [27,28], thermoacoustic oscillations [29,30], local extinction [29,31,32] and flashback [30,33]. Non-premixed flames are particularly sensitive to roll-up as their location depends on the transport processes in the diffusive layers [34]. If a flame (premixed or non-premixed) is weak enough and the vortex residence time in the flame is long enough, it can be considerably lengthened and rolled up, which leads to an increase in global heat release and could cause local flame extinction due to excessive strain an curvature induced by the vortex [12,13,35].

Combustion oscillations are amplified through a feedback loop between the combustion processes and the acoustic oscillations. Hence, in order to dampen these oscillations, the coupling between

* Corresponding author.
E-mail address: m.talibi@ucl.ac.uk (M. Talibi).

https://doi.org/10.1016/j.ijft.2020.100057

Nomenclature

C_2H_4	Ethylene
FDF	Flame Describing Function
fps	Frames Per Second
H_2	Hydrogen
LST	Laser Sheet Tomography
N_2	Nitrogen
NOx	Nitrogen oxides
OH^*	Hydroxyl radical
PMT	Photo Multiplier Tube
PSD	Power Spectral Density
Φ_{Global}	Global equivalence ratio
p	pressure
u	velocity
Q	heat release
FL	flame contour length

the oscillatory heat release and acoustic perturbations needs to be disrupted, which alters the phase relation between the two sets of oscillations, leading to a decay in their amplitudes [1,2,36]. Combustion instability can be reduced through passive and active control methods. Passive control methods, as outlined in [3], involve modifications to the hardware, such as modifying the fuel-air feed channel length [37], changing the bluff body shape [38] or altering the combustor geometry [39,40], which have been shown to be quite effective. However, these methods are only effective over a limited range of frequencies and operating conditions, and the modifications can be quite costly and time-consuming. Active control methods, on the other hand, provide a more dynamic approach to controlling oscillations by introducing an actuator that provides a closed-loop response to sensors placed in the combustion chamber. The actuator dynamically modifies parameters in response to measured signals, resulting in a more effective approach to decoupling acoustic and heat release oscillations.

One common approach of active control is the dynamic introduction of fuel close to the base of the flame, also known as secondary fuel addition or pilot injection, to create a localised richer zone. This changes the local equivalence ratio, and the resulting variation in flame dynamics alters the phase relation between the heat release and acoustic pressure modulation. Several experimental [41–50] and numerical [51–54] studies have been conducted to understand the impact of secondary fuel addition on combustion oscillations. Emris and Whitelaw [44] investigated low frequency oscillations in turbulent natural gas flames and observed that redirecting a small quantity of fuel from the main flow to a secondary injector, placed close to the combustor entrance, reduced the pressure oscillations and improved the overall stability of the flame. However, this improvement was only observed within a narrow range of operating conditions. Marzouk et al. [52] numerically showed that the addition of methane (as secondary fuel) to methane-air flames had a significant impact on the combustion process, including reaction zone broadening, burning rate enhancement, and flammability limit extension towards leaner mixtures. The spatial gradients of radical concentration and temperature produced by the unsteady equivalence ratio mixtures provided the flame with the ability to burn at leaner mixtures. In the work carried out by Albrecht et al. [46], secondary fuel injectors placed at the flame base and at the combustor dump plane were used to locally introduce fuel and vary the overall equivalence ratio. The authors reported a reduction in pressure oscillations and NOx emissions, and concluded that this was mainly achieved by the high jet momentum of the secondary injectors. In addition, the combined fuel injections prevented lift-off of the main flame, which appeared to be another damping source for the pressure perturbations.

The studies presented above utilise the same fuel for both primary and secondary injection. The use of alternative gases as secondary fuel to curtail combustion oscillations has received considerable attention in the recent past. Hydrogen (H_2) is one such potential fuel; blends of hydrocarbon fuels and hydrogen have been reported to significantly improve flame stability and ignitability [48,55–59]. The addition of H_2 increases the lean limit of operation, reducing the risk of flame blow-off, which is a common problem in lean premixed combustors [38,60–63]. Recent works [56,64,65] have also reported considerable reductions in heat release perturbations as a result of H_2 addition, attributable to the higher burning velocity of H_2. However, findings from Wicksall and Agrawal [66] demonstrated that their premixed flame exhibited strong instabilities with H_2 addition. Chen [67] also concluded that the addition of H_2 to methane-air flames could destabilise the flame.

Hydrogen is also preferred as a fuel as it does not produce carbon emissions, however it does increase flame temperatures which could augment NOx production. H_2 addition results in higher reaction rates, which expands the size of the reaction zones making the recirculation zones smaller. This reduces the availability of the relatively cooler gases, leading to an increase in the global temperature, and thus enhancing the production of NOx [57,64,65,68–70]. However, several studies have reported appreciable reductions in NOx emissions with H_2 addition [45,66,71]. This was speculated to be due to the addition of H_2 allowing the flame to burn at ultra-lean conditions, hence significantly reducing the global flame temperatures and curtailing NOx production.

While hydrogen enrichment does have a promising role in the development of future low-emission combustion technologies, it can be seen from the review of literature that researchers who have conducted investigations of H_2 addition within the context of combustion instability and NOx reduction have reported contradictory results. In addition, the effect of H_2 on combustion oscillations is not very well understood. Recent advances in fuel-flexible gas turbines offers the possibility to use other gases for secondary injection to mitigate instabilities. This work will investigate the effect of the local addition of various gases (fuels and diluent) to turbulent imperfectly-premixed self-excited ethylene flames. The specific objectives of this work are to study the effectiveness of the following methods in reducing combustion instabilities: (i) fuel-splitting, that is supplying part of the primary fuel via secondary fuel ports, ii) local H_2 addition and iii) local addition of N_2 (diluent). The following sections of the paper provide details of the experimental hardware and testing methodology employed, followed by results and discussion on the effect of the local addition of the three gases, and summary of the key findings from this study.

2. Experimental methodology

2.1. Combustor

A bluff body stabilised combustor, the design of which is based on Ref. [72] was employed for this study. The schematic of the combustor is shown in Fig. 1(a). The plenum had an internal diameter (ID) of 100 *mm* and a total length of 300 *mm*, with divergent and convergent cross sections at the inlet and exit of the plenum which prevented any flow separation during the expansion and contraction of the gas. The flow was streamlined using a section of honeycomb mesh placed as a flow straighter. The plenum delivers the mixture to the combustion chamber via a long duct with an ID of 35 *mm* and length 400 *mm*. This enables acoustic pressure measurements for the two-microphone method. The pressure fluctuations in the flow at the inlet to the combustion chamber were measured using two high-sensitivity pressure transducers (KuLite model XCS-093, sensitivity 4.2857×10^{-3} mV/Pa). The signals from the transducers were amplified using a

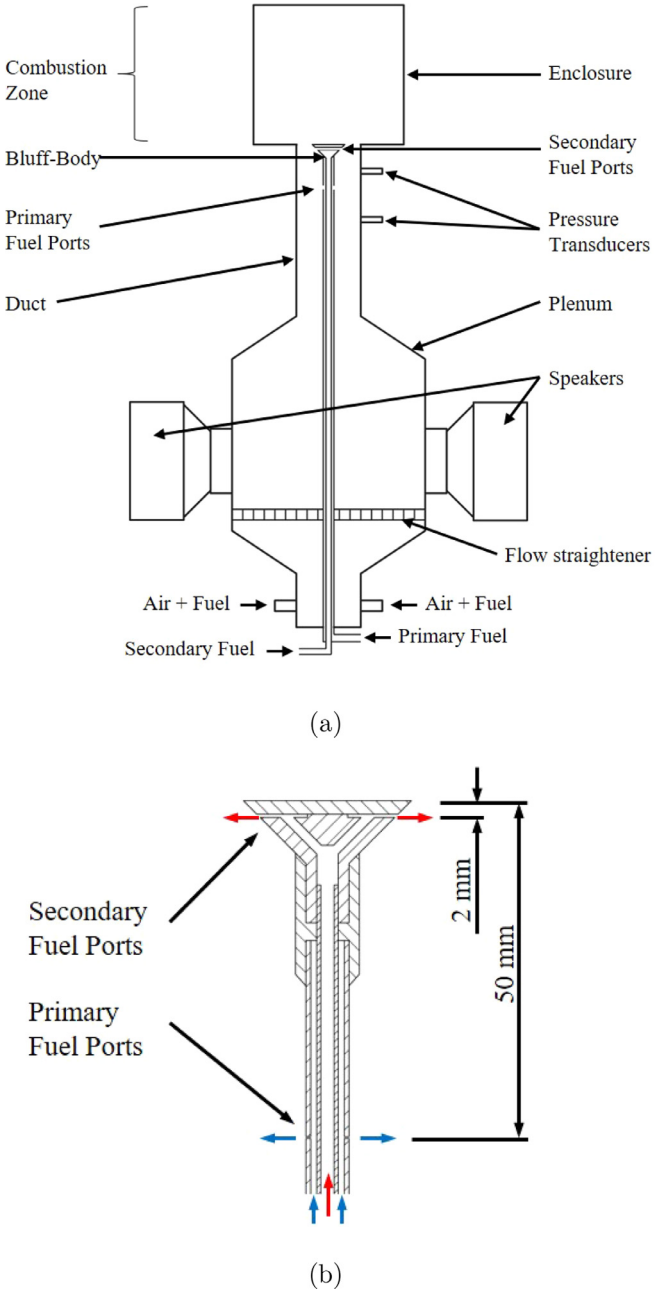

Fig. 1. (a) Schematic of the combustor assembly, (b) Sectional view of the bluff-body, showing the primary and secondary fuel ports.

Flyde Micro Analogue amplifier and acquired onto a PC using National Instruments data acquisition systems.

The bluff body used in for this study was conical in shape Fig. 1(b), with a diameter of 25 *mm*, resulting in a blockage ratio of 50%. As shown in Fig. 1(b), the bluff body had two provisions of introducing fuel into the air stream, either via the primary fuel ports (six holes, each of diameter 0.25 *mm*, placed circumferentially on the main fuel pipe) or using the secondary injection ports, which are six 2 *mm* ports placed 2 *mm* below the burner. This configuration allows for three different modes of operation: (1) fully premixed mode fuel and air mixed completely before entering the combustor, (2) imperfectly-premixed mode fuel introduced a short distance upstream of the flame (via the primary fuel ports) to achieve partial premixing and (3) local addition (from the secondary fuel ports) with either of the above modes (see Fig. 1(b)). Two long concentric tubes were welded to the bluff body which served as fuel supply lines for the two injection ports. In this study, due to possibility of flame flashback during self-excitation under fully premixed conditions, only imperfectly-premixed flames were considered. The combustion zone of the combustor was enclosed using a combination of quartz and stainless steel cylinders of internal diameter 70 *mm*, and a combined length of 300 *mm*. The bottom section of the enclosure, of length 100 *mm*, was made of quartz for optical diagnostics, while the rest was stainless steel. The enclosure prevented local equivalence ratio fluctuations due to air entrainment from the surroundings. The air was delivered from a central compressor while the other gases were supplied from compressed gas cylinders. The flow rates of all the gases were controlled using digital mass flow meters (Red-Y Smart), which has an accuracy of $\pm$ 1.5% of the full-scale reading.

2.2. Optical diagnostic arrangement

The layout of the optical diagnostic facility is shown in Fig. 2. High speed light sheet tomography (LST) or simply laser tomography was used to identify the boundary between the reactants and burnt products to extract a 2-D flame contour, as described in [73]. The tomography setup included a Pegasus laser (532 *nm*, maximum frequency 10,000 *Hz*) and a Photron high-speed camera (maximum rate 20,000 frames per second-fps). The laser beam was expanded into a laser sheet to illuminate a region of 12.5 x 12.5 *mm*, with a flame height of 2.5 - 15 *mm* from the base of the combustor being captured. The flow was seeded with fine olive oil droplets and the Mie scattering was captured using the high-speed camera at 3000 fps. Discriminating intensity levels of Mie scattering from unburnt region to virtually none in burnt region allowed identification of the boundary between the unburnt reactants and burnt combustion products. The flame contour thus evaluated from this method were used to produce time-series snapshots of the evolution of the flame length (which is indicative of the flame surface area).

OH^* chemiluminescence was measured using a Hamamatsu side-on photo-multiplier tube (PMT) fitted with an interference filter which had a center wavelength of 307 *nm* and bandpass of $\pm$ 10 *nm*.

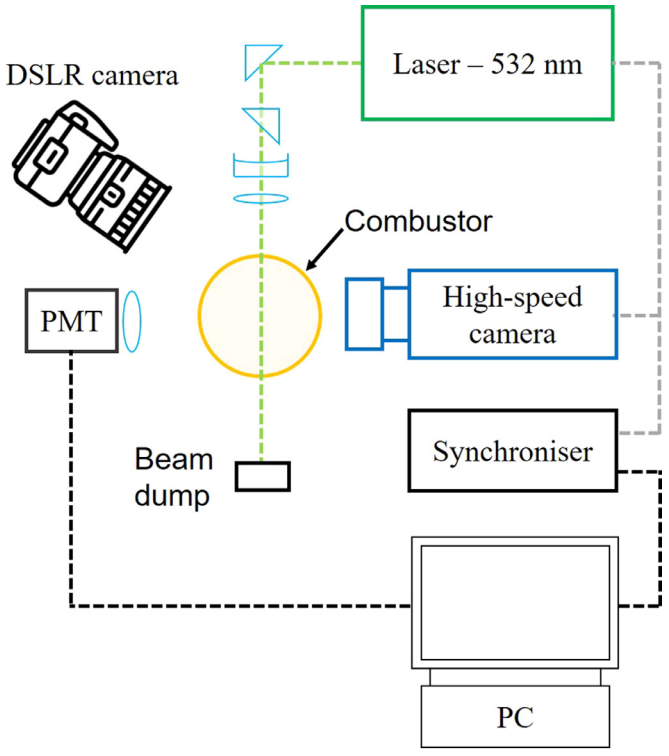

Fig. 2. Setup of the optical diagnostic system.

A plano-convex lens was also mounted in front of the PMT which focused the entire flame on the PMT collection window. Data was recorded at a sample rate of 10,000 *Hz* over a period of 2 seconds using National Instruments data acquisition software. A DSLR camera was also used to capture photographic images of the flames to show differences in their general appearance. The DSLR camera was set at a fixed position, aperture size, shutter speed, ISO and white balance to allow the comparison between flame images of different flow conditions.

2.3. Flow conditions

The following procedure was utilised to achieve self-excitation of the imperfectly-premixed ethylene flames. The flow rate of air was fixed at 250 *slpm*, and the air-fuel mixture was ignited at a global equivalence ratio at which the flame is not acoustically self-excited, that is, no dominant frequency is observed on the power spectrum (please note, the global equivalence ratio is based on the air and fuel flow rates and does not take into account the extent of premixedness of the air/fuel mixture). The flow rate of ethylene was then increased until the amplitude of the pressure oscillations exhibited a significant increase, and a clear dominant frequency was observed on the power spectrum. In the current work, self-excitation was observed at a global equivalence ratio, Φ_{Global}, of 0.812.

As described before, this work will investigate the effect of local addition of gases in order to control acoustic oscillations. Table 1 shows the flow conditions used for the local addition of the three secondary gases, (a) ethylene, (b) hydrogen (H_2) and (c) nitrogen (N_2) to imperfectly-premixed ethylene flames. The three gases were introduced through the secondary fuel ports of the bluff body (see Fig. 1 (b)). Ethylene was added to investigate whether fuel stratification could help reduce combustion oscillations. Hydrogen and nitrogen were added to understand the effect of diluents, both reactive (H_2) and inert (N_2), on heat release fluctuations. Several parameters were kept constant in order to enable comparison between the three secondary gases. The air flow rate was fixed at 250 *slpm*. The input power, calculated from the calorific value of the fuel mixture, was kept constant at 13.11 kW. The momentum ratio, defined by the Eqn. (1) (where sec denotes the secondary gas added, while pri represents the primary mixture of ethylene and air), was kept constant between the three secondary gases, for each flow condition, in order maintain the same level of penetration of each locally added gas (ethylene, hydrogen and nitrogen) in the primary ethylene-air flow. This was done by adjusting the volume flow rates of hydrogen and nitrogen, so that they matched the momentum ratio of the locally added ethylene, as can be seen in Tab. 1.

$$Momentum\ ratio = \frac{\rho_{sec}.{\mu_{sec}}^2}{\rho_{pri}.{\mu_{pri}}^2} \tag{1}$$

Table 1
Experimental flow conditions for the local addition of (a) ethylene, (b) hydrogen and (c) nitrogen to imperfectly-premixed turbulent ethylene flames.

(a)

Air (slpm)	Primary C_2H_4 (slpm)	Primary C_2H_4 %	Secondary H_2 (slpm)	Secondary H_2 %	Φ_{Global}	Momentum Ratio
250.0	14.2	100.0	0.0	0.0	0.812	0.00000
250.0	14.1	95.0	0.7	5.0	0.812	0.00065
250.0	13.9	90.0	1.5	10.0	0.811	0.00283
250.0	13.6	80.0	3.4	20.0	0.809	0.01370
250.0	13.2	70.0	5.7	30.0	0.808	0.03799

(b)

Air (slpm)	Primary C_2H_4 (slpm)	Primary C_2H_4 %	Secondary C_2H_4 (slpm)	Secondary C_2H_4 %	Φ_{Global}	Momentum Ratio
250.0	14.2	100.0	0.0	0.0	0.812	0.00000
250.0	14.0	98.6	0.2	1.4	0.812	0.00065
250.0	13.8	97.1	0.4	2.9	0.812	0.00283
250.0	13.3	93.6	0.9	6.4	0.812	0.01370
250.0	12.7	89.4	1.5	10.6	0.812	0.03799

(c)

Air (slpm)	Primary C_2H_4 (slpm)	Primary C_2H_4 %	Secondary N_2 (slpm)	Secondary N_2 %	Φ_{Global}	Momentum Ratio
250.0	14.2	100.0	0.0	0.0	0.812	0.00000
250.0	14.2	98.6	0.2	1.4	0.812	0.00065
250.0	14.2	97.2	0.4	2.8	0.812	0.00283
250.0	14.2	94.0	0.9	6.0	0.812	0.01370
250.0	14.2	90.3	1.5	9.7	0.812	0.03799

3. Data analysis

3.1. Global heat release fluctuation

Both the pressure and the OH* chemiluminescence signals had a cyclic response under the dominant acoustic excitation. The pressure transducer signals were analysed using the two-microphone technique to calculate the velocity fluctuation, u', and normalised by bulk velocity, $\langle U \rangle$, at the inlet to the combustion chamber, as detailed in the following references [72,74]. The flame describing function, *FDF*, (also known as the non-linear flame transfer function, *NFTF*) was determined from the ratio of the heat release fluctuations and the velocity perturbations, $FDF(f, u'/\langle U \rangle) = \left(Q'(f)/\langle Q \rangle\right)/(u'/\langle U \rangle)$. The normalised values of $\langle OH* \rangle$ were used to represent the heat release fluctuation, $Q'(f)/\langle Q \rangle$.

3.2. Image processing

Flame images were captured using the high-speed tomography setup for a duration of 100 *ms*. The flame contour was obtained by post processing the images through various steps of filtration, binarization and tracing the flame boundary, to obtain a single pixel thick flame front. The flame contour length (*FL*) was taken to be indicative of the flame surface area. Fig. 3 shows the region of the flame captured with the laser tomography technique, which was 12.5 *mm* wide and 12.5 *mm* in height (from 2.5 *mm* to 15 *mm* downstream of the base of the combustor). Similar to the OH* chemiluminescence, the flame contour length was also put through FFT and the power spectral density (PSD) was calculated, which was then normalised with the averaged flame length $\langle FL \rangle$ to obtain $FL'(f)/\langle FL \rangle$.

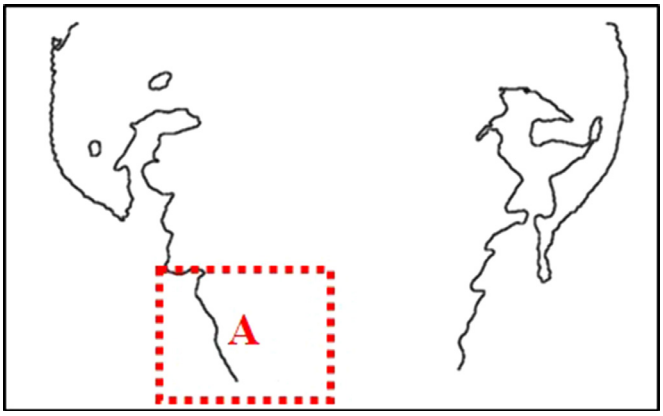

Fig. 3. Region of interest on a flame front image.

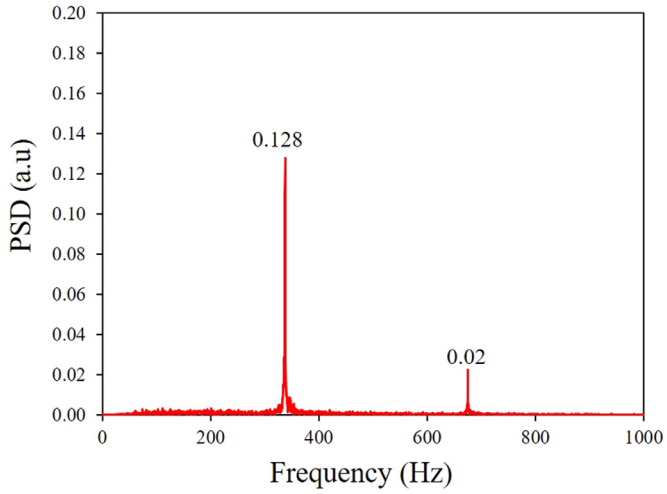

Fig. 4. Power spectral density (PSD) plot of the OH* chemiluminescence for self-excited imperfectly-premixed ethylene flames.

4. Results and discussion

4.1. Self-exited ethylene combustion

Fig. 4 shows the power spectral density (PSD) plot, generated by applying fast Fourier transform (FFT) on the OH* chemiluminescence signal, for self-excited imperfectly-premixed ethylene flames with no local addition, that is, the base test case (see Tab. 1). The PSD plot shows a sharp peak at 338 *Hz*, clearly demonstrating that this is the dominant self-excitation frequency. Fig. 5(a) shows the time-series plot for the flame surface area, while Fig. 5(b) shows the power spectrum obtained from the time-series data to determine the frequency at which the flame surface area fluctuations were taking place. Significant fluctuations in the flame surface area, with peak-to-peak values of about 1-1.5, close to the base of the combustor can be observed in Fig. 5(a), which was observed to cause roll-up of the flame front. The PSD plot (Fig. 5(b)) shows that the frequency of the flame surface area fluctuations is 340 *Hz*, which is very close (barring experimental inaccuracies) to the dominant frequency of oscillations from the OH* signal (Fig. 4). Hence, this

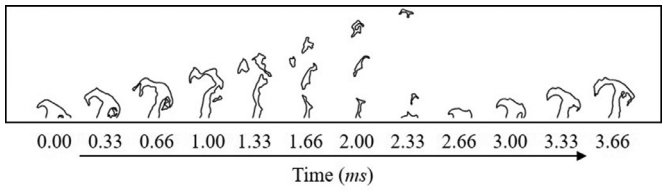

Fig. 6. Time series evolution of the flame boundary of the self-excited imperfectly-premixed ethylene flames, without local addition of secondary gases (Φ_{Global}=0.812).

confirms that the heat release oscillations can be captured by the flame surface modulation.

The time-series of images in Fig. 6 depict the flame-vortex interactions, particularly the evolution of the coherent structures during self-excited oscillations for imperfectly-premixed ethylene flames, without any local addition of secondary gases. The instances of the flame were captured every 0.33 *ms* and the images show periodic formation, and subsequent destruction, of flame vortices. It is clear from the images that the appearance of coherent structures corresponded with the least amount of flame element, and it is likely that this point would have coincided with the trough of the flame contour length (5 (a)). The coherent structures continue to convect upstream, which would potentially contribute to an increase in the heat release oscillations, followed by complete disintegration of the flame structures.

4.2. Effect of fuel-splitting on the dynamics of self-excited ethylene flames

The effectiveness of fuel-splitting, that is, splitting part of the primary fuel and adding it locally to turbulent imperfectly-premixed ethylene flames, in reducing combustion oscillations was investigated. For these set of tests, the overall equivalence ratio was kept the same, while the fuel flow rates in the two fuel streams (via the primary and secondary ports) were varied - see Tab. 1. Fig. 7 presents photographs of the flame with increasing percentage of the local addition of ethylene as a secondary fuel. It can be observed in Fig. 7 that as the amount of secondary ethylene is increased, the flames become increasingly yellow and sooty. This is most likely due to the poor mixing of the locally added ethylene with the primary flow air, creating a locally rich mixture and resulting in unburnt

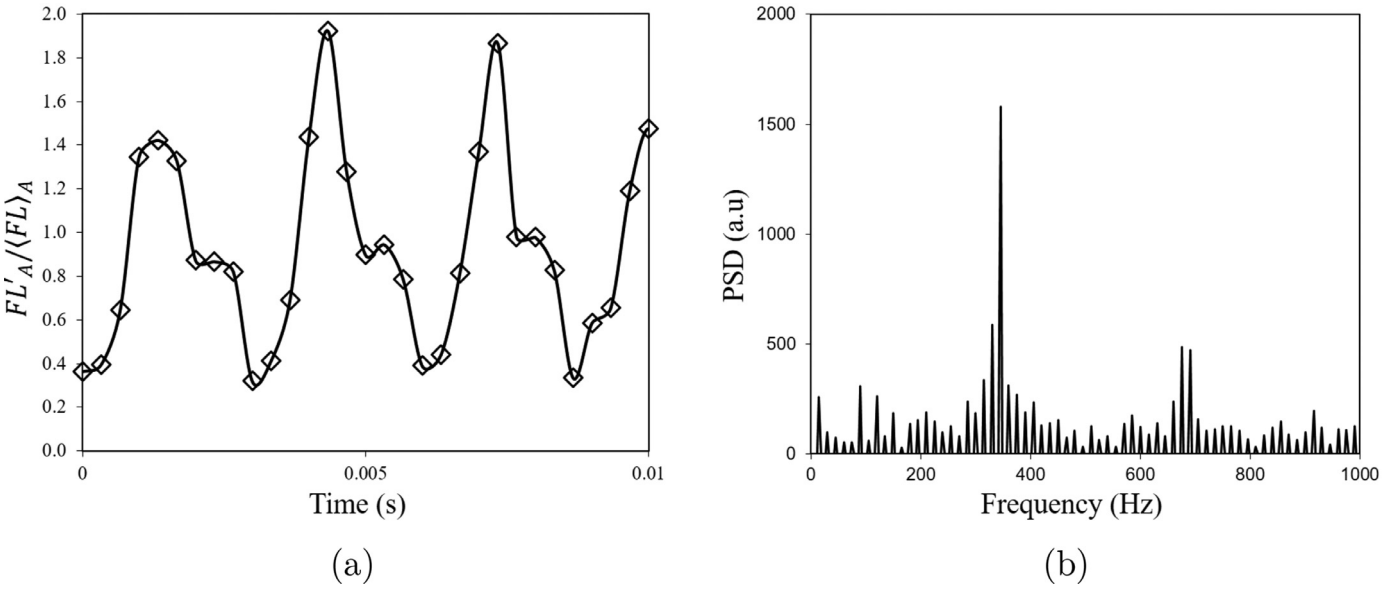

Fig. 5. (a) Time series plot of the flame contour length (indicative of flame surface area) determined by laser tomography, which was processed to produce the (b) power spectral density (PSD) plot.

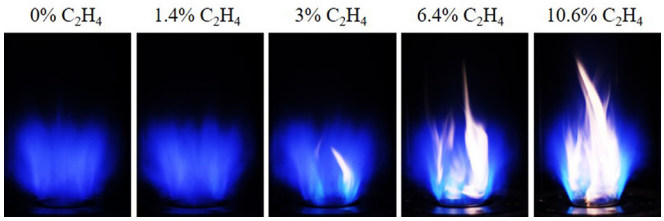

Fig. 7. Photographic images of the self-excited imperfectly-premixed ethylene flame with local addition of ethylene through secondary fuel ports.

hydrocarbons, and the consequent high soot formation. The observed soot formation could result in inaccurate estimates (due to broad black-body radiation from soot) of the heat release from the readings of the OH* chemiluminescence using the PMT. Furthermore, these soot rich areas caused bright spots in the tomography imaging. Hence, for the local addition of ethylene, only changes in the velocity perturbations were determined from the pressure measurements, and both normalised pressure and velocity oscillations have been shown in Fig. 8. It can be seen in Fig. 8 that when 1.4% of ethylene (by volume) is removed from the primary flow and injected locally through the secondary ports, the pressure and velocity perturbations increase. However, subsequent addition of ethylene through the secondary ports (and removal from the primary), results in considerable reductions in the velocity oscillations. The initial increase in the perturbations could be attributed to the increase in the local equivalence ratios towards stoichiometric values as a result of the local addition of small amounts of ethylene (up to 1.4%), which would increase the local premixedness, and hence contribute to an increase in the heat release. Further addition of ethylene would have made the local equivalence ratios rich (as evidenced by the appearance of soot in the flame photographs), which would result in decreased flame temperatures and a reduction in the magnitude of oscillations.

4.3. Local addition of hydrogen to self-excited ethylene flames

The results from the tests carried out to understand the effectiveness of local addition of hydrogen for combustion instability control have been presented in this section. H_2 was added via the secondary fuel ports during the self-excited oscillations of imperfectly-premixed ethylene flames. The effects of H_2 addition on pressure, velocity and heat release perturbations, and on the flame describing function, have been shown in Fig. 9. It can be observed from the figure that the addition of up to 10% H_2 results in a significant reduction in the normalised velocity oscillations (Fig. 9(b)), however subsequent H_2 addition does not show any appreciable change. A similar trend is observed for the heat release response, that is, a reduction of almost 60% when 10% H_2 is added, with no change observed beyond 10% H_2 addition (Fig. 9(c)). The flame describing function (Fig. 9(d)), determined from the velocity and heat release fluctuation data, exhibits a decreasing reduction with H_2 addition. This reduction in the pressure perturbations is consistent with the findings reported by Barbosa et al. [64], who investigated the local addition of H_2 as an instability control technique. In order to explain this reduction, the authors [64] captured phase locked images of OH* and CH*, which showed that the hydrogen jet breaks the coupling between the acoustic and heat release oscillations.

The power spectra calculated from global OH* chemiluminescence and the flame length estimates are shown in Fig. 10(a) and Fig. 10(b), respectively. The magnitude of the PSD based on the OH* chemiluminescence signal and from the flame contour length (*FL*) show a significant reduction in the peak of the dominant frequency when the H_2 addition is increased upto 10%. Beyond 10% H_2 addition, both PSD plots exhibit minimal changes with increasing H_2 addition. Both these observations correlate well with the trends in pressure and velocity perturbations observed in Fig. 9. Considering the time-based evolution of the flame boundary images shown in Fig. 11 for 5% and 20% H_2 addition, it is apparent that an increase in the local addition of H_2 leads to an overall increase in the flame contour length. Even at the lowest point of the heat release, the flame elements disintegrate to a lesser degree with increasing H_2 addition. It could be speculated that the reduction in the velocity and heat release perturbations with H_2 addition, observed in Fig. 9, are due to this increase in the flame contour length and the lesser extent of flame destruction. Some evidence for this can be seen in time series plots of the heat release fluctuations, presented in the Appendix (Figure A.1, A.2 and A.3), which show a reduction in the troughs with H_2 addition. The minimal change seen in the magnitude of PSD (Fig. 10) at 20% and 30% H_2 addition could be attributed to flame annihilation

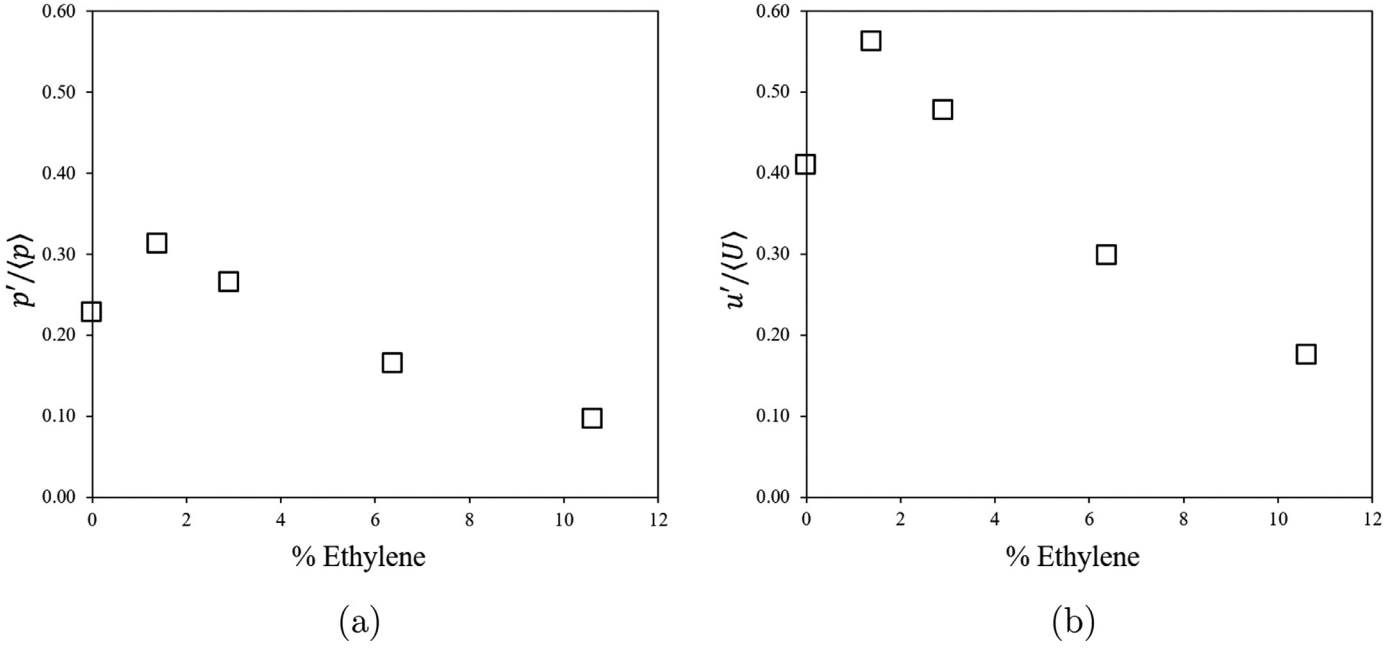

Fig. 8. Variation in the normalised (a) pressure and (b) velocity perturbations of self-excited imperfectly-premixed ethylene flames with an increase in the local addition of ethylene.

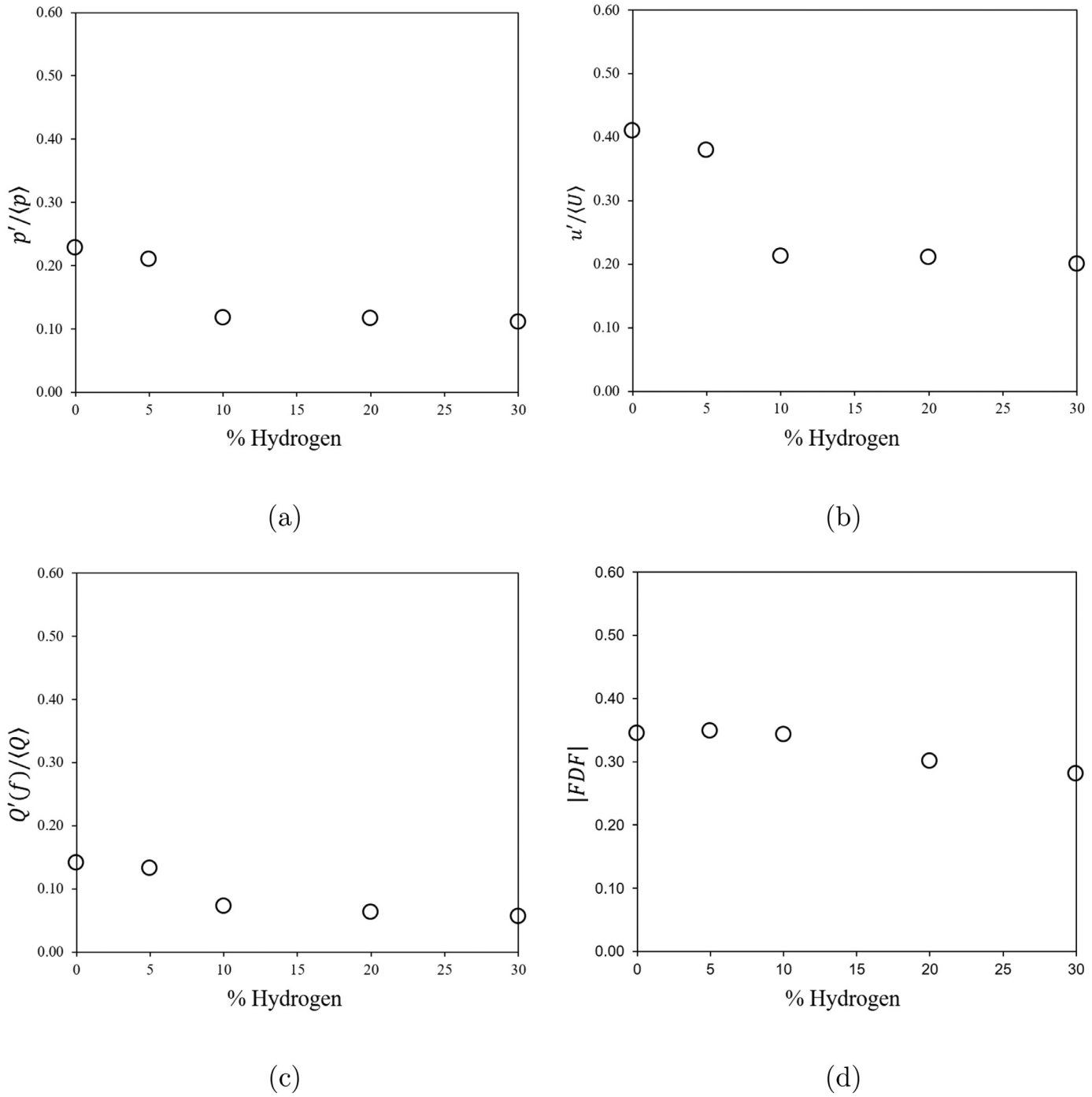

Fig. 9. Variation in the normalised (a) pressure, (b) velocity, (c) heat release perturbations and the magnitude of the flame describing function of self-excited imperfectly-premixed ethylene flames with an increase in the local addition of hydrogen.

becoming a self-limiting factor, with no further flame destruction possible with increasing H_2 addition. This can be observed in Fig. 11(c) which shows instantaneous images of the flame boundary with different H_2 addition for self-excited ethylene flames. Due to flame-vortex interaction in the inner recirculation zone a large part of the flame gets annihilated (as shown by the regions circled in red), and as H_2 is added beyond 20% the vortex is not able to cause any further flame roll-up.

4.4. Addition of nitrogen to self-excited ethylene flames

The local addition of nitrogen (N_2), via the secondary fuel ports, to self-excited ethylene flames was carried out as a control. N_2 is inert and does not contribute energy to the combustion process, thereby acting primarily as a diluent. It is clearly evident that the flame boundary images shown in Fig. 12 for 9.7% N_2 addition are largely similar to those for pure ethylene flames (Fig. 6). Fig. 13 compares the time-series plots of the flame length for pure ethylene and ethylene/9.7% nitrogen, and only an insignificant reduction in the peaks and troughs of the surface area can be observed with N_2 addition, which shows that the added N_2 had a negligible impact on the flame roll-up occurrence in the self-excited flames. Fig. 14 shows the normalised velocity and heat release oscillations for up to 9.7% (by volume) N_2 addition, while the power spectra calculated from global OH* chemiluminescence and the flame length estimates are shown in Fig. 15(a) and Fig. 15(b), respectively. No effect of N_2 addition can be observed in Fig. 14 and Fig. 15, except for a slight increase in the perturbations at 1.4% N_2 addition. Although it is

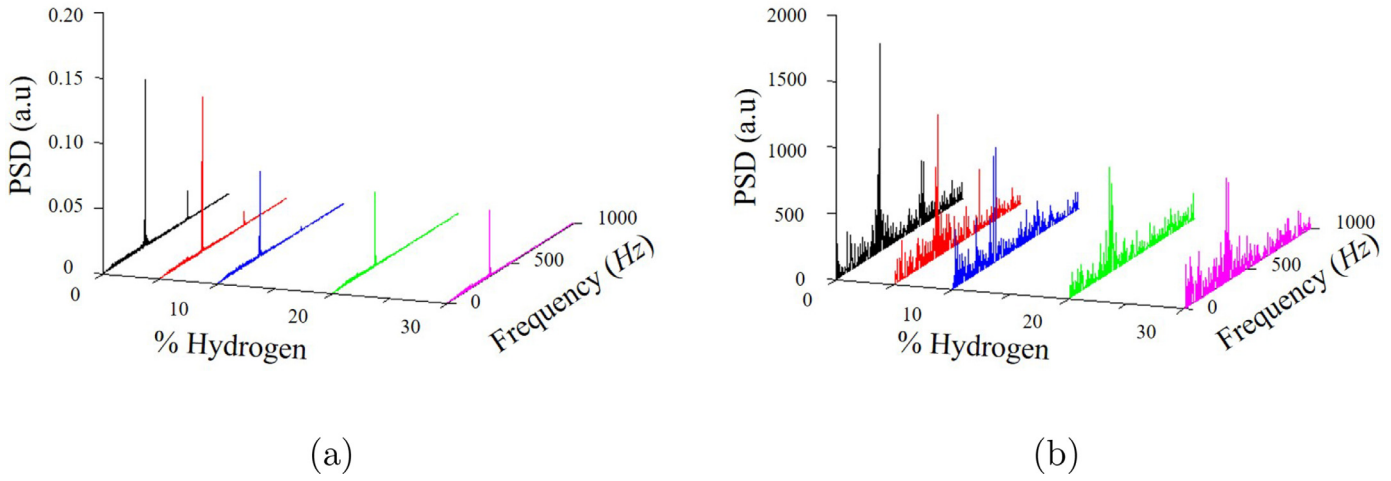

Fig. 10. Power spectral density (PSD) plots calculated from (a) the global OH* chemiluminescence, and (b) flame contour length (indicative of flame surface area), for the self-excited ethylene flames with 0, 5, 10, 20 and 30% local addition of hydrogen.

known that the addition of N_2 reduces the flame temperature, it is speculated that the level of N_2 added in this work was too low to have any appreciable impact.

The observations with N_2 also confirm that the effects observed with ethylene and H_2 addition are primarily due to them taking part in the combustion reaction, and not because of these gases acting as a diluent in the combustion mixture.

5. Conclusions

This study investigated the effect of the local addition of three secondary gases, ethylene, hydrogen and nitrogen, to imperfectly-premixed self-excited ethylene flames. The secondary gas flow rates were adjusted to keep the momentum ratio between the secondary gas and the primary ethylene/air fuel mixture constant and match the level of penetration each secondary gas had into the main

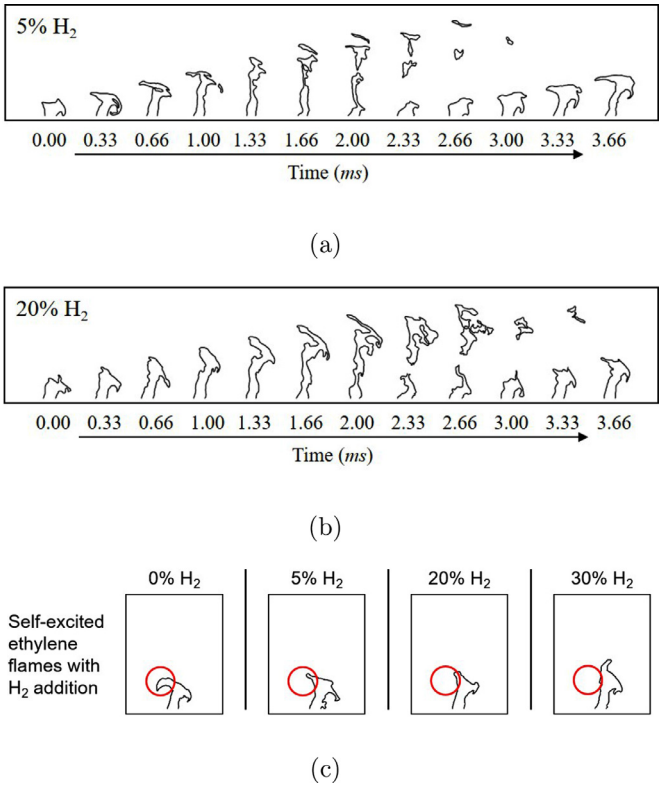

Fig. 11. Images showing the temporal evolution of the flame boundary for the self-excited imperfectly-premixed ethylene flames with (a) 5% and (b) 20% local addition of hydrogen, while (c) compares the initial development of the flame roll-up of the same flames with different H_2 addition.

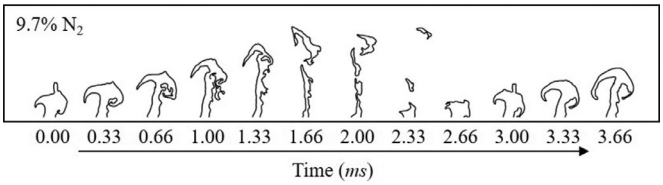

Fig. 12. Images showing the evolution of the flame boundary of self-excited imperfectly-premixed ethylene flames with 9.7% local addition of nitrogen.

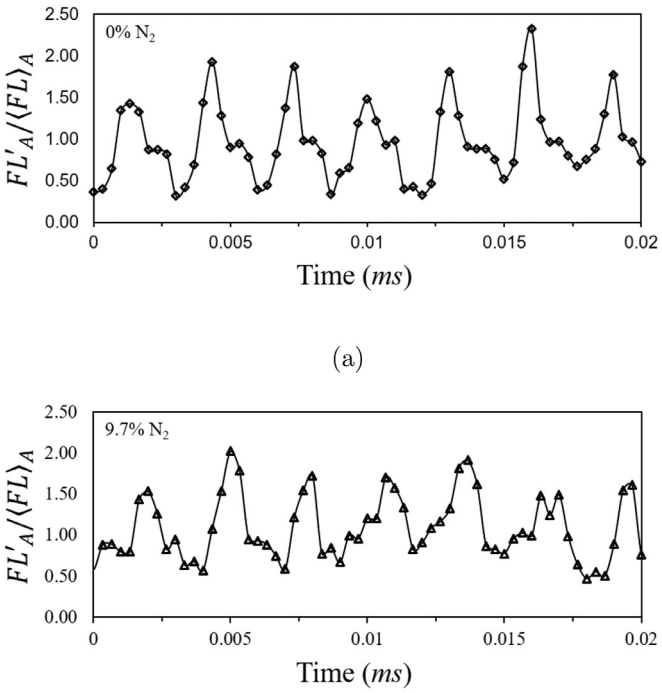

Fig. 13. Time series plots of the flame contour length (indicative of flame surface area) for (a) pure ethylene and (b) ethylene 9.7% nitrogen self-excited flames.

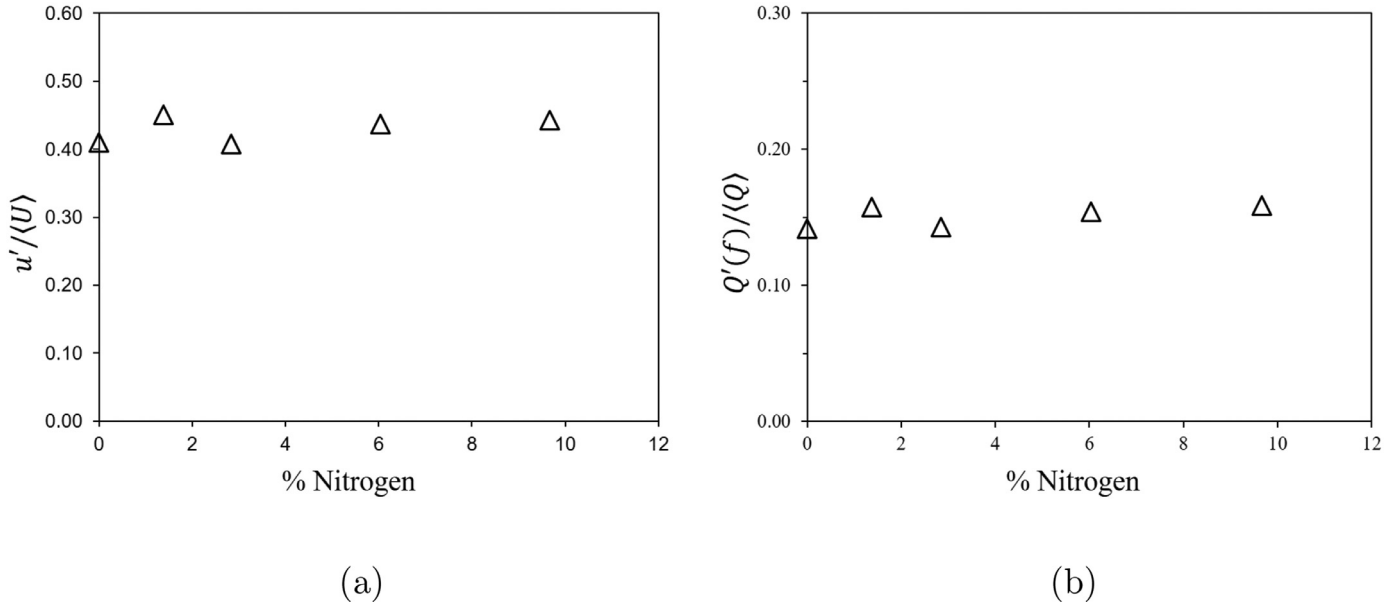

Fig. 14. Variation in the (a) normalised velocity perturbations and (b) global normalised heat release fluctuations of self-excited imperfectly-premixed ethylene flames with increasing local addition of nitrogen.

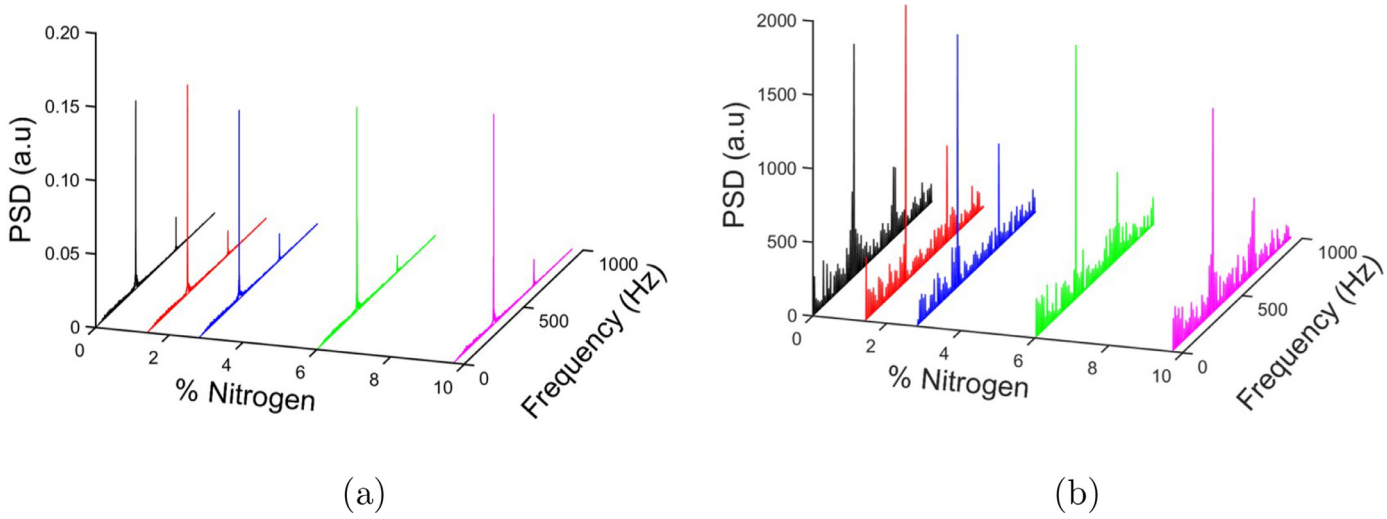

Fig. 15. Power spectral density (PSD) plots calculated from (a) the global OH* chemiluminescence, and (b) flame contour length (indicative of flame surface area), for the self-excited ethylene flames with 0, 1.4, 2.8, 6.0 and 9.7% local addition of nitrogen.

(primary) flow. In addition, the combined calories of the combustible mixture (primary and secondary) was also kept constant by reducing the main ethylene flow as the secondary gas flow was increased.

The self-excited ethylene flames experienced a recurring oscillation of pressure, velocity and heat release, accompanied by a periodic formation and destruction of the flame roll-up in the region close to the base of the combustor. The addition of H_2 reduced the pressure, velocity and heat release perturbations, and decreased the initial size of the flame roll-up. However, these effects were only observed for up to 10% H_2 addition, subsequent H_2 addition (of up to 30%) did not exhibit any appreciable changes beyond that level.

The local addition of ethylene (to observe the effects of fuel-splitting), of up to 2.9%, resulted in an increase in the normalised pressure and velocity oscillations. Higher levels of ethylene addition (beyond 2.9%) reduced the magnitude of oscillations, however the flame became increasingly yellow, indicating the presence of soot and unburnt hydrocarbons, and hence lower combustion efficiency. No noticeable change in the velocity and heat release perturbations, and in the flame surface area fluctuations was observed with the addition of nitrogen, leading to the conclusion that the thermal dilution effect of N_2 was not significant enough to alter the dynamical flame response.

Hence, it can be concluded from this work that the local addition of H_2 is most effective in reducing the degree of perturbations of self-excited ethylene flames, and that is attributed to the disruption of the coupling between heat release and acoustic oscillations. For the operating parameters tested in this work, the local addition of gaseous fuel (ethylene) and inert gas (nitrogen) was not observed to be as effective in controlling combustion instability. This approach of secondary addition of hydrogen not only is able to mitigate combustion instabilities but has the potential to keep emissions low (through lean burn operation) and achieve higher efficiency.

Declaration of Competing Interest

The authors declare that they have no known competing financial interests or personal relationships that could have appeared to influence the work reported in this paper.

Acknowledgment

The authors would like to acknowledge Siemens Industrial Turbomachinery Ltd. Lincoln, UK and EPSRC (EP/P003036/1 and EP/G063788/1) for their support towards this work.

Appendix A

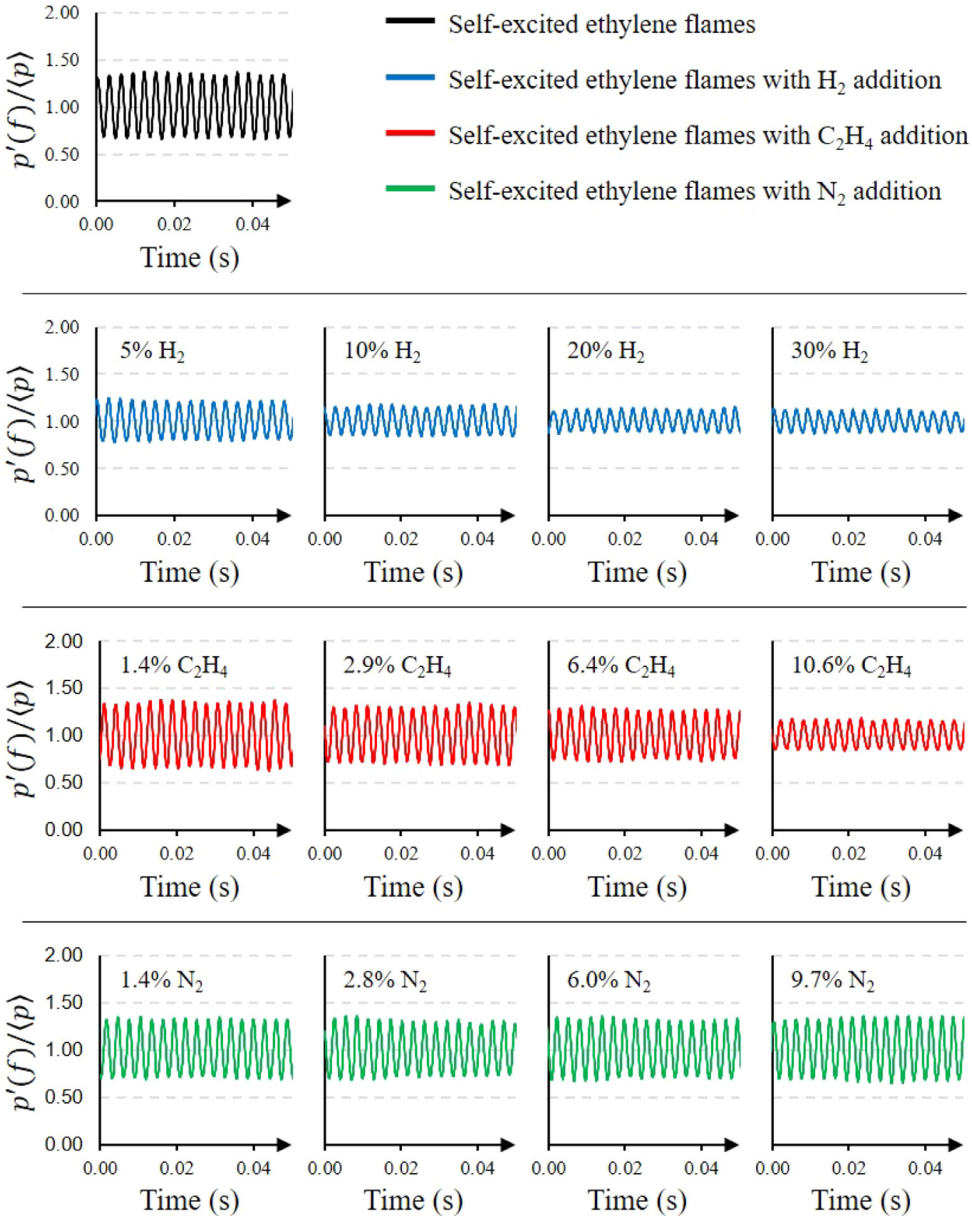

Fig. A.1. Time series plots of normalised pressure fluctuations for ethylene self-excited flames, with the local addition of H_2, C_2H_4 and N_2.

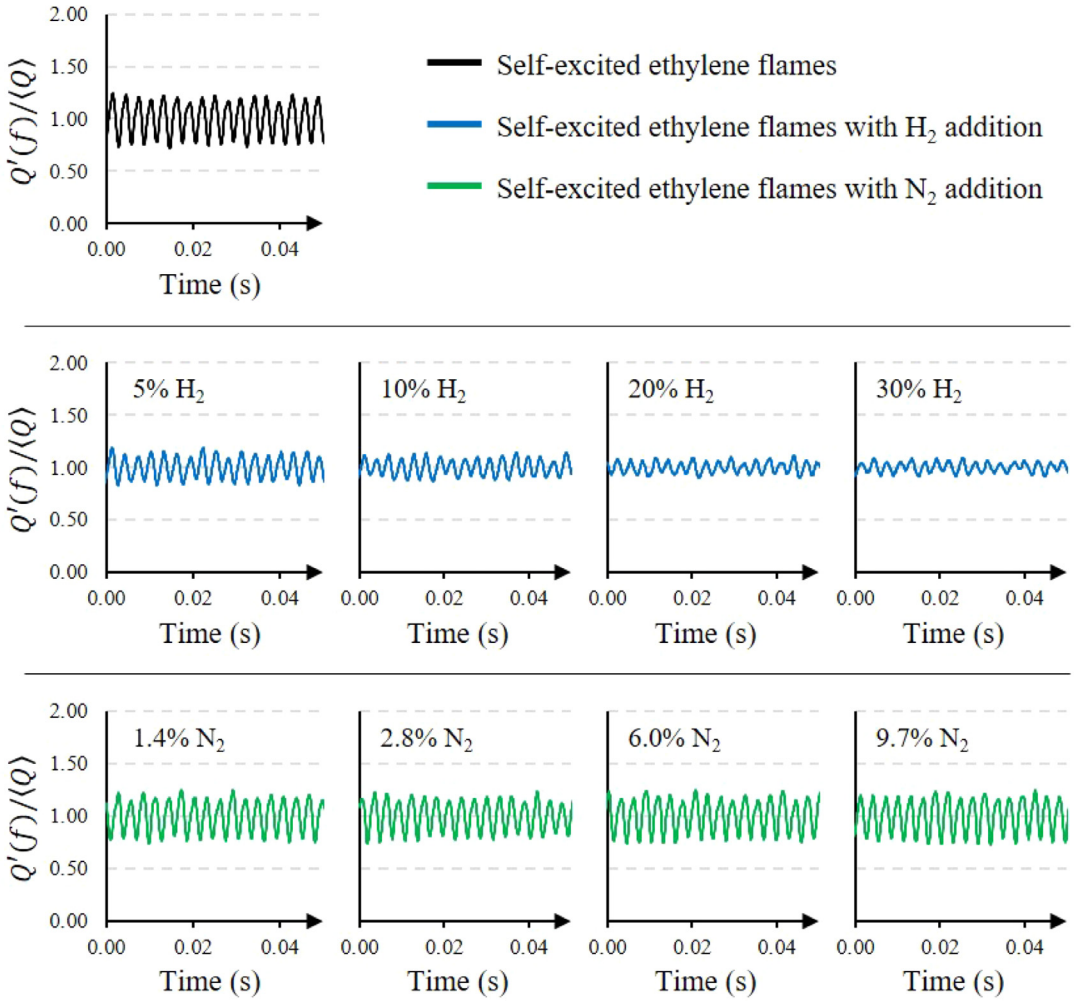

Fig. A.2. Time series plots of normalised heat release fluctuations evaluated from OH* chemiluminescence, for ethylene self-excited flames, with the local addition of H_2 and N_2.

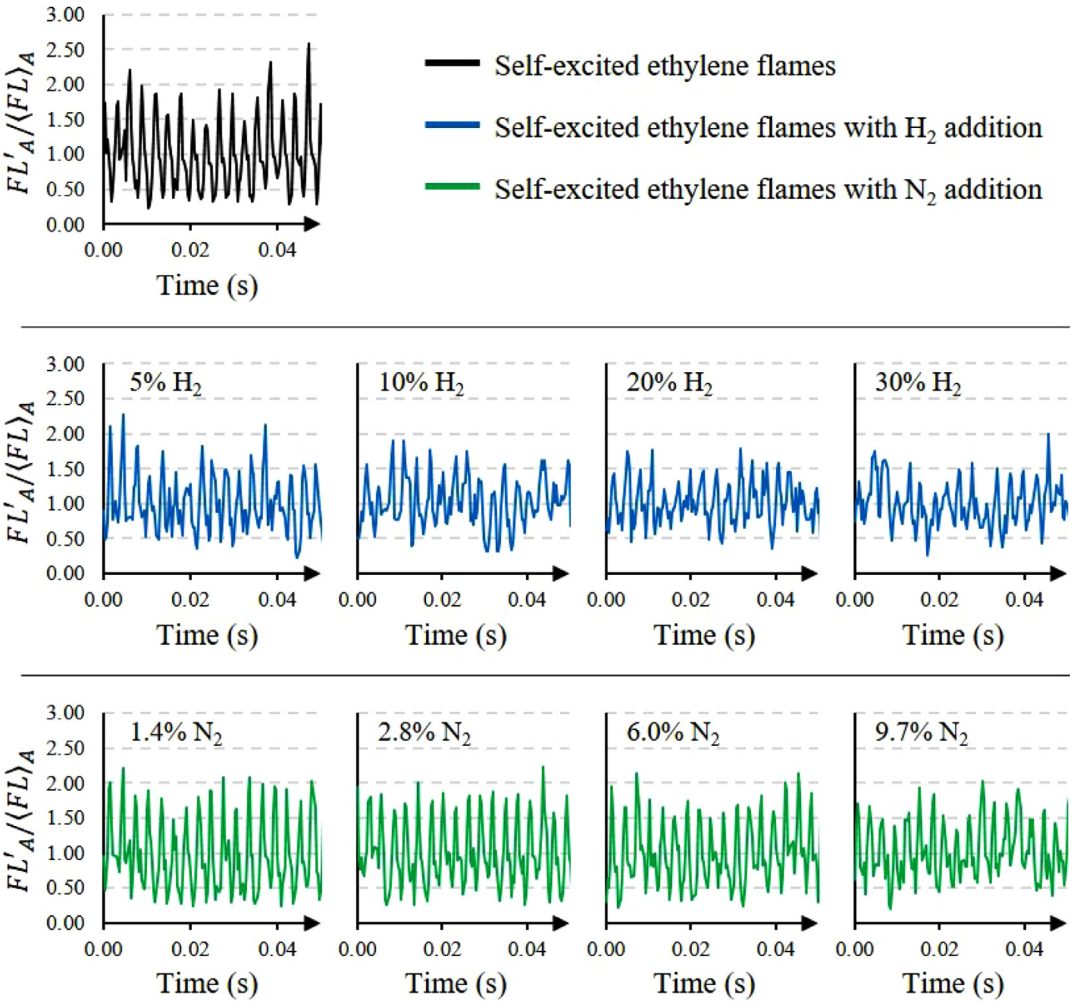

Fig. A.3. Time series plots of normalised flame contour length, for ethylene self-excited flames, with the local addition of H_2 and N_2.

References

[1] S. Candel, Combustion dynamics and control: progress and challenges, Proc. Combust. Inst. 29 (1) (2002) 1–28, doi: 10.1016/S1540-7489(02)80007-4.

[2] A.P. Dowling, A.S. Morgans, Feedback control of combustion oscillations, Annu Rev Fluid Mech 37 (1) (2005) 151–182, doi: 10.1146/annurev.fluid.36.050802.122038.

[3] T.C. Lieuwen, V. Yang, Combustion instabilities in gas turbine engines, American Institute of Aeronautics and Astronautics, Reston, VA, 2006, doi: 10.2514/4.866807.

[4] L. Jiang, C. Gu, G. Zhou, F. Li, Q. Wang, Cellular instabilities of n-butane/air flat flames probing by PLIF-OH and PLIF-CH2O laser diagnosis, Exp. Therm Fluid Sci. 118 (2020) 110155.

[5] O. Agwu, A. Valera-Medina, Diesel/syngas co-combustion in a swirl-stabilised gas turbine combustor, International Journal of Thermofluids 3-4 (2020) 100026, doi: 10.1016/j.ijft.2020.100026.

[6] T.C. Lieuwen, Investigation of combustion instability mechanisms in premixed gas turbines, Georgia Institute of Technology, 1999 Ph.D. thesis.

[7] F. Blomshield, Historical perspective of combustion instability in motors - case studies, 37th Joint Propulsion Conference and Exhibit, American Institute of Aeronautics and Astronautics, Reston, Virigina, 2001, doi: 10.2514/6.2001-3875.

[8] G. Lartigue, U. Meier, C. Bérat, Experimental and numerical investigation of self-excited combustion oscillations in a scaled gas turbine combustor, Appl Therm Eng 24 (11–12) (2004) 1583–1592.

[9] A.A. Putnam, Combustion-driven oscillations in industry, New York : American Elsevier Pub. Co, 1971.Includes bibliographies

[10] T. Smith, B. Emerson, W. Proscia, T. Lieuwen, Role of induced axial acoustics in transverse acoustic flame response, Combust Flame 195 (2018) 140–150 ISSN 0010-2180, doi: 10.1016/j.combustflame.2017.12.035.

[11] K. Ma, X. Yu, X. Zhao, X. Li, S. Li, D. Zhao, B. Shi, Response of lean premixed swirl tubular flame to acoustic perturbations, Exp. Therm Fluid Sci. (2020) 110199.

[12] P.-H. Renard, D. Thevenin, J.-C. Rolon, S. Candel, Dynamics of flame/vortex interactions, Prog Energy Combust Sci 26 (3) (2000) 225–282.

[13] D. Thevenin, P.-H. Renard, G. Fiechtner, J.R. Gord, J.-C. Rolon, Regimes of non-premixed flame-vortex interactions, Technical Report, Laboratoire EM2C CNRS Ecole Centrale Paris and CNRS Chetaney-Malabry (France), 2000.

[14] T. Lieuwen, Modeling premixed combustion-acoustic wave interactions: a review, J. Propul. Power 19 (5) (2003) 765–781.

[15] G. Wang, X. Liu, X. Xia, S. Wang, F. Qi, Dynamics of periodically-excited vortices in swirling flames, Proc. Combust. Inst. (2020) ISSN 1540-7489, doi: 10.1016/j.proci.2020.06.308.

[16] T. Meyer, G. Fiechtner, S. Gogineni, J.-C. Rolon, C. Carter, J.R. Gord, Simultaneous plif/piv investigation of vortex-induced annular extinction in h 2-air counterflow diffusion flames, Exp Fluids 36 (2) (2004) 259–267.

[17] A. Lemaire, T. Meyer, K. Zähringer, J.R. Gord, J.-C. Rolon, Piv/plif investigation of two-phase vortex–flame interactions: effects of vortex size and strength, Exp Fluids 36 (1) (2004) 36–42.

[18] M. Tanahashi, S. Murakami, G.-M. Choi, Y. Fukuchi, T. Miyauchi, Simultaneous ch–oh plif and stereoscopic piv measurements of turbulent premixed flames, Proc. Combust. Inst. 30 (1) (2005) 1665–1672.

[19] D. Wicksall, A. Agrawal, R. Schefer, J. Keller, The interaction of flame and flow field in a lean premixed swirl-stabilized combustor operated on h2/ch4/air, Proc. Combust. Inst. 30 (2) (2005) 2875–2883.

[20] R. Sadanandan, M. Stöhr, W. Meier, Simultaneous oh-plif and piv measurements in a gas turbine model combustor, Appl. Phys. B 90 (3–4) (2008) 609–618.

[21] M. Stöhr, R. Sadanandan, W. Meier, Experimental study of unsteady flame structures of an oscillating swirl flame in a gas turbine model combustor, Proc. Combust. Inst. 32 (2) (2009) 2925–2932.

[22] M. Stöhr, R. Sadanandan, W. Meier, Phase-resolved characterization of vortex–flame interaction in a turbulent swirl flame, Exp Fluids 51 (4) (2011) 1153–1167.

[23] C. Mueller, J. Driscoll, D. Sutkus, W. Roberts, M. Drake, M. Smooke, Effect of unsteady stretch rate on oh chemistry during a flame-vortex interaction: to assess flamelet models, Combust Flame 100 (1–2) (1995) 323–331.

[24] C.J. Mueller, J.F. Driscoll, D.L. Reuss, M.C. Drake, M.E. Rosalik, Vorticity generation and attenuation as vortices convect through a premixed flame, Combust Flame 112 (3) (1998) 342–358.

[25] J. Hult, U. Meier, W. Meier, A. Harvey, C. Kaminski, Experimental analysis of local flame extinction in a turbulent jet diffusion flame by high repetition 2-d laser techniques and multi-scalar measurements, Proc. Combust. Inst. 30 (1) (2005) 701–709.

[26] P. Kothnur, M. Tsurikov, N. Clemens, J. Donbar, C.D. Carter, Planar imaging of ch, oh, and velocity in turbulent non-premixed jet flames, Proc. Combust. Inst. 29 (2) (2002) 1921–1927.

[27] S. Chaudhuri, S. Kostka, M.W. Renfro, B.M. Cetegen, Blowoff dynamics of bluff body stabilized turbulent premixed flames, Combust Flame 157 (4) (2010) 790–802.

[28] S. Chaudhuri, S. Kostka, S.G. Tuttle, M.W. Renfro, B.M. Cetegen, Blowoff mechanism of two dimensional bluff-body stabilized turbulent premixed flames in a prototypical combustor, Combust Flame 158 (7) (2011) 1358–1371.

[29] I. Boxx, M. Stöhr, C. Carter, W. Meier, Temporally resolved planar measurements of transient phenomena in a partially pre-mixed swirl flame in a gas turbine model combustor, Combust Flame 157 (8) (2010) 1510–1525.

[30] A.M. Steinberg, I. Boxx, M. Stöhr, C.D. Carter, W. Meier, Flow–flame interactions causing acoustically coupled heat release fluctuations in a thermo-acoustically unstable gas turbine model combustor, Combust Flame 157 (12) (2010) 2250–2266.

[31] B. Böhm, C. Heeger, I. Boxx, W. Meier, A. Dreizler, Time-resolved conditional flow field statistics in extinguishing turbulent opposed jet flames using simultaneous highspeed piv/oh-plif, Proc. Combust. Inst. 32 (2) (2009) 1647–1654.

[32] N.A. Worth, J.R. Dawson, Characterisation of flame surface annihilation events in self excited interacting flames, Combust Flame 199 (2019) 338–351.

[33] M. Konle, F. Kiesewetter, T. Sattelmayer, Simultaneous high repetition rate piv–lif-measurements of civb driven flashback, Exp Fluids 44 (4) (2008) 529–538.

[34] P.-H. Renard, J.C. Rolon, D. Thévenin, S. Candel, Investigations of heat release, extinction, and time evolution of the flame surface, for a nonpremixed flame interacting with a vortex, Combust Flame 117 (1–2) (1999) 189–205.

[35] J. Park, H.D. Shin, Experimental investigation of the developing process of an unsteady diffusion flame, Combust Flame 110 (1–2) (1997) 67–77.

[36] K. McManus, T. Poinsot, S. Candel, A review of active control of combustion instabilities, Prog Energy Combust Sci 19 (1) (1993) 1–29, doi: 10.1016/0360-1285(93)90020-F.

[37] Y. Zhang, X. Liu, D. Che, et al., Numerical study of the self-excited thermoacoustic vibrations occurring in combustion system, Appl Therm Eng 160 (2019) 113994.

[38] G. Bagheri, S.E. Hosseini, M.A. Wahid, Effects of bluff body shape on the flame stability in premixed micro-combustion of hydrogen–air mixture, Appl Therm Eng 67 (1–2) (2014) 266–272.

[39] K. Schadow, E. Gutmark, Combustion instability related to vortex shedding in dump combustors and their passive control, Prog Energy Combust Sci 18 (2) (1992) 117–132, doi: 10.1016/0360-1285(92)90020-2.

[40] N. Tran, S. Ducruix, T. Schuller, Damping combustion instabilities with perforates at the premixer inlet of a swirled burner, Proc. Combust. Inst. 32 (2) (2009) 2917–2924, doi: 10.1016/j.proci.2008.06.123.

[41] M.S. Mansour, Y.-C. Chen, N. Peters, Highly strained turbulent rich methane flames stabilized by hot combustion products, Combust Flame 116 (1–2) (1999) 136–153, doi: 10.1016/S0010-2180(98)00029-7.

[42] S.S. Sattinger, Y. Neumeier, A. Nabi, B.T. Zinn, D.J. Amos, D.D. Darling, Sub-scale demonstration of the active feedback control of gas-turbine combustion instabilities, J Eng Gas Turbine Power 122 (2) (2000) 262, doi: 10.1115/1.483204.

[43] S. Nair, T. Lieuwen, Acoustic detection of imminent blowout in pilot and swirl stabilized combustors, Volume 2: Turbo Expo 2003, ASME, 2003, pp. 55–65, doi: 10.1115/GT2003-38074.

[44] I. Emiris, J.H. Whitelaw, Control of combustion oscillations, Combust. Sci. Technol. 175 (1) (2003) 157–184, doi: 10.1080/00102200302363.

[45] H. Guo, B. Tayebi, C. Galizzi, D. Escudié, Burning rates and surface characteristics of hydrogen-enriched turbulent lean premixed methane-air flames, Int J Hydrogen Energy 35 (20) (2010) 11342–11348, doi: 10.1016/j.ijhydene.2010.07.066.

[46] P. Albrecht, S. Bade, A. Lacarelle, C.O. Paschereit, E. Gutmark, Instability control by premixed pilot flames, J Eng Gas Turbine Power 132 (4) (2010) 041501, doi: 10.1115/1.3019293.

[47] C. Galizzi, D. Escudié, Experimental analysis of an oblique turbulent flame front propagating in a stratified flow, Combust Flame 157 (12) (2010) 2277–2285, doi: 10.1016/j.combustflame.2010.07.008.

[48] H. Kim, V. Arghode, A. Gupta, Flame characteristics of hydrogen-enriched methane-air premixed swirling flames, Int J Hydrogen Energy 34 (2) (2009) 1063–1073, doi: 10.1016/j.ijhydene.2008.10.035.

[49] K. Kim, S. Hochgreb, The nonlinear heat release response of stratified lean-premixed flames to acoustic velocity oscillations, Combust Flame 158 (12) (2011) 2482–2499, doi: 10.1016/j.combustflame.2011.05.016.

[50] S. Balusamy, L.K. Li, Z. Han, S. Hochgreb, Extracting flame describing functions in the presence of self-excited thermoacoustic oscillations, Proc. Combust. Inst. 36 (3) (2017) 3851–3861.

[51] D. Bradley, Premixed turbulent flame instability and NO formation in a lean-burn swirl burner, Combust Flame 115 (4) (1998) 515–538, doi: 10.1016/S0010-2180(98)00024-8.

[52] Y. Marzouk, A. Ghoniem, H. Najm, Dynamic response of strained premixed flames to equivalence ratio gradients, Proc. Combust. Inst. 28 (2) (2000) 1859–1866, doi: 10.1016/S0082-0784(00)80589-5.

[53] V. Robin, A. Mura, M. Champion, O. Degardin, B. Renou, M. Boukhalfa, Experimental and numerical analysis of stratified turbulent V-shaped flames, Combust Flame 153 (1–2) (2008) 288–315, doi: 10.1016/j.combustflame.2007.10.008.

[54] K. Nogenmyr, P. Petersson, X. Bai, C. Fureby, R. Collin, A. Lantz, M. Linne, M. Aldén, Structure and stabilization mechanism of a stratified premixed low swirl flame, Proc. Combust. Inst. 33 (1) (2011) 1567–1574, doi: 10.1016/j.proci.2010.06.011.

[55] R. Schefer, D. Wicksall, A. Agrawal, Combustion of hydrogen-enriched methane in a lean premixed swirl-stabilized burner, Proc. Combust. Inst. 29 (1) (2002) 843–851, doi: 10.1016/S1540-7489(02)80108-0.

[56] H. Kim, V. Arghode, M. Linck, A. Gupta, Hydrogen addition effects in a confined swirl-stabilized methane-air flame, Int J Hydrogen Energy 34 (2) (2009) 1054–1062, doi: 10.1016/j.ijhydene.2008.10.034.

[57] A. Mardani, S. Tabejamaat, Effect of hydrogen on hydrogen-methane turbulent non-premixed flame under MILD condition, Int J Hydrogen Energy 35 (20) (2010) 11324–11331, doi: 10.1016/j.ijhydene.2010.06.064.

[58] M. Reyes, F.V. Tinaut, A. Horrillo, A. Lafuente, Experimental characterization of burning velocities of premixed methane-air and hydrogen-air mixtures in a constant volume combustion bomb at moderate pressure and temperature, Appl Therm Eng 130 (2018) 684–697.

[59] N. Castro, M. Toledo, G. Amador, An experimental investigation of the performance and emissions of a hydrogen-diesel dual fuel compression ignition internal combustion engine, Appl Therm Eng 156 (2019) 660–667.

[60] F. Cozzi, A. Coghe, Behavior of hydrogen-enriched non-premixed swirled natural gas flames, Int J Hydrogen Energy 31 (6) (2006) 669–677, doi: 10.1016/j.ijhydene.2005.05.013.

[61] C. Mandilas, M. Ormsby, C. Sheppard, R. Woolley, Effects of hydrogen addition on laminar and turbulent premixed methane and isooctane-air flames, Proc. Combust. Inst. 31 (1) (2007) 1443–1450, doi: 10.1016/j.proci.2006.07.157.

[62] M.S. Day, X. Gao, J.B. Bell, Properties of lean turbulent methane-air flames with significant hydrogen addition, Proc. Combust. Inst. 33 (1) (2011) 1601–1608, doi: 10.1016/j.proci.2010.05.099.

[63] N. Striūgas, K. Zakarauskas, R. Paulauskas, R. Skvorčinskienė, Chemiluminescence-based characterization of tail biogas combustion stability under syngas and oxygen-enriched conditions, Exp. Therm Fluid Sci. (2020) 110133.

[64] S. Barbosa, M. de La Cruz Garcia, S. Ducruix, B. Labegorre, F. Lacas, Control of combustion instabilities by local injection of hydrogen, Proc. Combust. Inst. 31 (2) (2007) 3207–3214, doi: 10.1016/j.proci.2006.07.085.

[65] S. El-Ghafour, A. El-dein, A. Aref, Combustion characteristics of natural gas-hydrogen hybrid fuel turbulent diffusion flame, Int J Hydrogen Energy 35 (6) (2010) 2556–2565, doi: 10.1016/j.ijhydene.2009.12.049.

[66] D. Wicksall, A. Agrawal, Acoustics measurements in a lean premixed combustor operated on hydrogen/hydrocarbon fuel mixtures, Int J Hydrogen Energy 32 (8) (2007) 1103–1112, doi: 10.1016/j.ijhydene.2006.07.008.

[67] Z. Chen, Effects of hydrogen addition on the propagation of spherical methane/air flames: a computational study, Int J Hydrogen Energy 34 (15) (2009) 6558–6567, doi: 10.1016/j.ijhydene.2009.06.001.

[68] A. Choudhuri, S. Gollahalli, Characteristics of hydrogen-hydrocarbon composite fuel turbulent jet flames, Int J Hydrogen Energy 28 (4) (2003) 445–454, doi: 10.1016/S0360-3199(02)00063-0.

[69] M. Ilbas, I. Yilmaz, Y. Kaplan, Investigations of hydrogen and hydrogen-hydrocarbon composite fuel combustion and emission characteristics in a model combustor, Int J Hydrogen Energy 30 (10) (2005) 1139–1147, doi: 10.1016/j.ijhydene.2004.10.016.

[70] J. Nam, J.J. Yoh, A numerical investigation of the effects of hydrogen addition on combustion instability inside a partially-premixed swirl combustor, Appl Therm Eng (2020) 115478.

[71] G. Dahl, F. Suttrop, Engine control and low-NOx combustion for hydrogen fuelled aircraft gas turbines, Int J Hydrogen Energy 23 (8) (1998) 695–704, doi: 10.1016/S0360-3199(97)00115-8.

[72] R. Balachandran, B. Ayoola, C. Kaminski, A. Dowling, E. Mastorakos, Experimental investigation of the nonlinear response of turbulent premixed flames to imposed inlet velocity oscillations, Combust Flame 143 (1) (2005) 37–55, doi: 10.1016/j.combustflame.2005.04.009.

[73] T. Chew, R. Britter, K. Bray, Laser tomography of turbulent premixed bunsen flames, Combust Flame 75 (2) (1989) 165–174, doi: 10.1016/0010-2180(89)90094-1.

[74] T. Schuller, D. Durox, S. Candel, Dynamics of and noise radiated by a perturbed impinging premixed jet flame, Combust Flame 128 (1) (2002) 88–110, doi: 10.1016/S0010-2180(01)00334-0.